

## Designed Glycopeptides with Different $\beta$ -Turn Types as Synthetic Probes for the Detection of Autoantibodies as Biomarkers of Multiple Sclerosis

Alfonso Carotenuto,<sup>†</sup> Maria Claudia Alcaro,<sup>‡,§,⊥</sup> Maria Rosaria Saviello,<sup>†</sup> Elisa Peroni,<sup>‡,§</sup> Francesca Nuti,<sup>‡,§</sup> Anna Maria Papini,<sup>‡,§</sup> Ettore Novellino,<sup>\*,†</sup> and Paolo Rovero<sup>\*,§,||</sup>

Department of Pharmaceutical and Toxicological Chemistry, University of Naples "Federico II", via D. Montesano 49, I-80131 Naples, Italy, and Departments of Organic Chemistry "Ugo Schiff" and Pharmaceutical Sciences and Laboratory of Peptide and Protein Chemistry and Biology, University of Florence, I-50019 Sesto Fiorentino, Italy

Received April 4, 2008

Circulating autoantibodies have been recognized as disease biomarkers of autoimmune diseases. We have previously disclosed a synthetic glycopeptide that is able to detect specific autoantibodies in sera of patients who are affected by multiple sclerosis (MS). This glycopeptide is characterized by a type I'  $\beta$ -turn around the minimal epitope Asn(Glc) that allows an efficient exposure of this moiety to antibody interactions in the context of a solid-phase immunoenzymatic assay. With the aim of optimizing the glycopeptide–antibody interactions, we analyze a series of new glycopeptides based on different turn structures. Our results confirm the role of conformation in the recognition and binding of synthetic antigenic probes to MS autoantibodies. Glycopeptide **2**, which is characterized by a type I  $\beta$ -turn around the minimal epitope Asn(Glc), shows the highest antibody affinity ( $IC_{50} = 11.8$  nM), and thus it appears to be a promising tool for the detection of specific autoantibodies as MS biomarker in patients' sera.

### Introduction

Although the role of circulating autoantibodies as disease biomarkers of autoimmune diseases, such as rheumatoid arthritis and systemic lupus erythematosus, is largely accepted,<sup>1</sup> the diagnostic/prognostic use of these valuable tools has been hampered by the limited availability of well-defined antigens (native, recombinant, or synthetic) to be used as immunological probes in simple and reproducible assays.<sup>2,3</sup>

We previously disclosed that a designed synthetic glycopeptide (CSF114(Glc), no. **1** in Table 1) is a valuable antigenic probe that is able to detect specific autoantibodies in sera of patients affected by multiple sclerosis<sup>a,4</sup> an inflammatory, demyelinating disease of the central nervous system that is elicited by an autoimmune mechanism against myelin antigens.<sup>5</sup> Glycopeptide **1** was developed starting from the observation that post-translational modifications of protein autoantigens, such as glycosylation, may play a fundamental role in autoimmunity.<sup>6</sup> Accordingly, this glycopeptide was selected as an efficient

**Table 1.** Glycopeptide Sequences

no.	peptide sequence
<b>1</b>	TPRVER N(Glc)GHSVFLAPYGWMVK
<b>2</b>	TPRVERPN(Glc)HT VFLAPYGWMVK
<b>3</b>	TPRVERGN(Glc)HT VFLAPYGWMVK
<b>4</b>	Ac-ERP(N)(Glc)HT V-NH <sub>2</sub>
<b>5</b>	Ac-RPN(Glc)HT-NH <sub>2</sub>

representation of pathogenetic autoantigens by the use of a reverse approach<sup>7</sup> based on the screening of focused peptide libraries on large collections of MS patients' sera, and it was subsequently used as an antigenic probe for the identification of MS-specific autoantibodies as disease biomarkers in a simple immunoenzymatic assay on patients' sera.<sup>8</sup>

A subsequent conformation–activity relationship study allowed us to define the structural requirements for the interaction of the glycopeptide antigens with specific autoantibodies.<sup>9</sup> We found that glycopeptides that were able to reveal high antibody titers in MS sera were characterized by a type I'  $\beta$ -turn around the previously identified minimal epitope Asn(Glc).<sup>4</sup> This peculiar conformational feature was found to be fundamental for an efficient exposure of the minimal epitope to antibody interactions in the context of a solid-phase immunoenzymatic assay.

In this article, we describe a conformationally driven rational design of new glycosylated synthetic probes derived from **1** with the aim of better understanding the role of the peptide structure in autoantibody recognition. In particular, because **1** is characterized by a  $\beta$ -hairpin motif with a type I'  $\beta$ -turn containing Asn<sup>7</sup> and Gly<sup>8</sup> as central residues,<sup>4,9</sup> we decided to investigate the role of the  $\beta$ -turn type in antibody recognition.

### Results

**Design of New Analogs.** In a previous work,<sup>4</sup> we established the ability of glycopeptides that bear the minimal epitope Asn(Glc) to detect autoantibodies in MS patients but not in healthy controls by using solid-phase ELISA. A conformation–

\* To whom correspondence should be addressed. (E.N.) Tel: +39-081-678646. Fax: +39-081-678644. E-mail: novellino@unina.it. (P.R.) Tel: +39-055-4573724. Fax: +39-055-4573584. E-mail: paolo.rovero@unifi.it.

<sup>†</sup> University of Naples.

<sup>‡</sup> University of Florence, Department of Organic Chemistry "Ugo Schiff".

<sup>§</sup> University of Florence, Laboratory of Peptide and Protein Chemistry and Biology.

<sup>||</sup> University of Florence, Department of Pharmaceutical Sciences.

<sup>⊥</sup> Current address: Toscana Biomarkers Srl, Siena, Italy.

<sup>a</sup> Abbreviations used for amino acids and the designation of peptides follow the rules of the IUPAC-IUB Joint Commission of Biochemical Nomenclature (*Eur. J. Biochem.* **1984**, *138*, 9–37). Amino acid symbols denote L configuration unless indicated otherwise. The following additional abbreviations are used: 1D, 2D, and 3D, one-, two-, and three-dimensional; DIPEA, *N,N*-diisopropylethyl amine; DQF-COSY, double quantum filtered correlation spectroscopy; ELISA, enzyme-linked immunosorbent assay; EM, energy minimization; Fmoc, 9-fluorenylmethoxycarbonyl; HFA, hexafluoroacetone; HOBt, *N*-hydroxybenzotriazole; MD, molecular dynamics; MS, multiple sclerosis; NOE, nuclear Overhauser effect; NMM, *N*-methylmorpholine; NOESY, nuclear Overhauser enhancement spectroscopy; TBTU, 2-(1H-benzotriazol-1-yl)-1,1,3,3-tetramethyluronium tetrafluoroborate; TOCSY, total correlated spectroscopy; TSP, 2,2,3,3-tetradeuterio-3-(trimethylsilyl)-propionic acid.

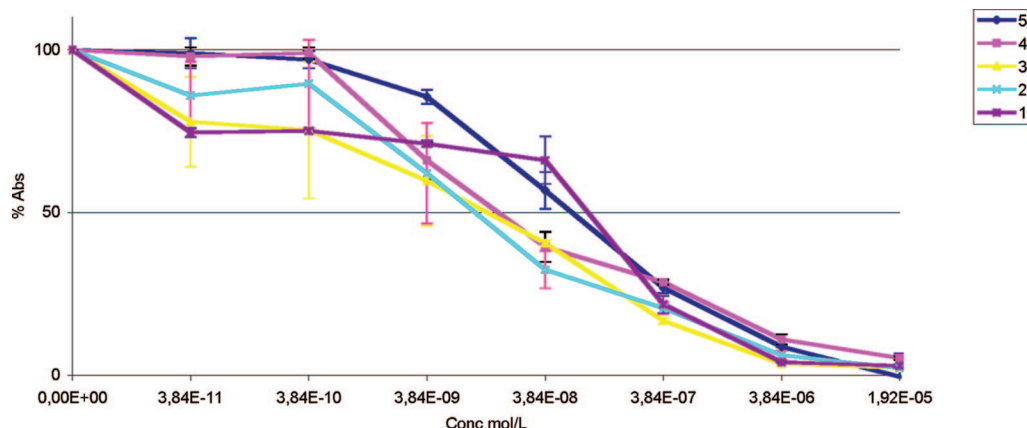


**Figure 1.** Inhibition curves of anti-CSF114(Glc) antibodies with glycopeptides **2–5** compared with **1** in a competitive ELISA. The results are expressed as the percentage of absorbance of a representative MS serum (ordinate axis). The concentrations of the peptides that are used as inhibitors are on the abscissa.

activity relationship study of these glycopeptides<sup>9</sup> revealed the role of conformation in the recognition and binding of MS autoantibodies in the solid-phase context of the immunoenzymatic assay. In particular, all of the glycopeptides that revealed high antibody titers in MS sera showed a type I  $\beta$ -turn around the minimal epitope Asn(Glc), which allows an efficient exposure of this moiety to autoantibody interactions. To explore the importance of the  $\beta$ -turn type in the glycopeptide–autoantibody interactions, we designed a focused library of new analogs (peptides **2–5**, Table 1). Starting from the sequence of **1**, we replaced the dipeptide at the tip of the  $\beta$ -turn, that is, Asn<sup>7</sup>–Gly<sup>8</sup>, with the sequence Pro<sup>7</sup>–Asn<sup>8</sup> and thus obtained peptide **2**. The latter sequence was chosen because it should stabilize a type I or type II  $\beta$ -turn as a result of the Pro and Asn residues that are found with high probability at positions  $i + 1$  and  $i + 2$ , respectively, of these  $\beta$ -turn types.<sup>10</sup> Following similar considerations, we replaced the sequence Asn<sup>7</sup>–Gly<sup>8</sup> with the sequence Gly<sup>7</sup>–Asn<sup>8</sup> in peptide **3**, which should stabilize a type II'  $\beta$ -turn. Because peptide **2** showed high affinity in MS autoantibody recognition (see below), we also synthesized two shorter sequences of this peptide: residues 5–11 (**4**) and 6–10 (**5**). These truncated sequences include the epitope region and should provide an understanding of the importance of the N- and C-terminal regions of the antigenic peptides. Finally, a Thr residue at position 10 was fixed for all of the new peptides, and thus we obtained the Asn–Xxx–Thr consensus sequence of the protein glycosylation sites.

**Synthesis of Glycopeptides.** The new glycopeptides were synthesized and purified as previously reported.<sup>11,12</sup> Briefly, syntheses were performed on the Liberty microwave peptide synthesizer (CEM, Matthews, NC) starting from Fmoc–Lys(Boc)–Wang resin for peptides **1–3** and from Rink amide resin for peptides **4** and **5**. A glucosyl moiety was introduced as the building block Fmoc–L–Asn[GlcOAc4]–OH, which was synthesized as previously reported.<sup>13</sup> All peptides were purified by semipreparative RPLC and were characterized by the use of analytical RPLC and ESIMS. Purification details and analytical data are reported in the Supporting Information.

**Multiple Sclerosis Autoantibodies Binding Affinities.** Competitive ELISA<sup>14</sup> was used to analyze the autoantibody binding affinities of the newly synthesized glycopeptides. The data shown in Figure 1 indicate that both [Pro<sup>7</sup>, Asn<sup>8</sup>(Glc), Thr<sup>10</sup>]CSF114 (**2**) and [Gly<sup>7</sup>, Asn<sup>8</sup>(Glc), Thr<sup>10</sup>]CSF114 (**3**) ( $IC_{50}$  = 11.8 and 30.3 nM, respectively) recognize autoantibodies with a higher affinity than does **1** ( $IC_{50}$  = 137 nM), which demonstrates that amino acid modifications in the proximity of

the minimal epitope may significantly affect autoantibody recognition. At variance, amino acid residues that are remote from the epitope appear to play a minor role. In fact, the heptapeptide analog of **2**, namely, glycopeptide **4**, maintains the same affinity as the parent peptide ( $IC_{50}$  = 14.9 nM), whereas the corresponding pentapeptide **5** shows an approximately 4-fold decrease in affinity ( $IC_{50}$  = 73.8 nM).

**Conformational Analysis.** The conformational behavior in a solution of peptides **2–4** was investigated by means of NMR spectroscopy. Nuclear magnetic resonance spectra were recorded in water and in HFA/water (50/50 v/v). It was reported that this solvent mixture is a stabilizing agent that increases the intrinsic tendency of the amino acid sequence to fold in defined secondary structures.<sup>15</sup> A whole set of 1D and 2D <sup>1</sup>H NMR spectra were acquired for all of the peptides. To check for the absence of an aggregation state of the peptides, we acquired spectra in the concentration range of 0.2–2 mM. No significant changes were observed in the distribution or in the shape of the <sup>1</sup>H NMR resonances, which indicates that no aggregation phenomena occurred in this concentration range. Complete <sup>1</sup>H NMR chemical shift assignments were effectively achieved (Supporting Information) according to the Wüthrich procedure<sup>16</sup> via the usual systematic application of DQF-COSY,<sup>17</sup> TOCSY,<sup>18</sup> and NOESY<sup>19</sup> experiments with the support of the XEASY software package.<sup>20</sup> Signal broadening in the HFA solution, which was probably due to solvent viscosity, hampered the measurement of scalar coupling constants in this environment.

Nuclear magnetic resonance analysis of **2** was performed in water at pH 5 and at 277.1 K. Almost all NMR parameters indicate structural flexibility: the almost complete lack of medium- and long-range NOEs as well as the observed high-temperature coefficients ( $\Delta\delta/\Delta T < -4.0$  ppb/K) for all of the backbone amide proton resonances clearly point to a random-coil state. Most of the <sup>3</sup> $J_{HN-H\alpha}$  coupling constants are within the range of 6–8 Hz, which again indicates random structures; only a few coupling constants are  $>8.0$  Hz (Val<sup>4</sup>, Glu<sup>5</sup>, Val<sup>11</sup>, and Leu<sup>13</sup>), which indicates that these residues are in extended conformations. A very weak  $d_{\alpha N}(i, i + 2)$  NOE observed between Pro<sup>7</sup> and His<sup>9</sup> indicates the presence of a population of structures that possesses a  $\beta$ -turn moiety that encompasses residues 6–9. The <sup>3</sup> $J_{\alpha N}$  coupling constant of Asn<sup>8</sup> residue (<sup>3</sup> $J_{\alpha N}$  = 7.9 Hz) points to a type I  $\beta$ -turn structure.  $H_{\alpha}$  resonances of residues 14–20 show downfield shifts compared with random-coil reference values,<sup>21</sup> which indicates the propensity of this segment for the helical structures. Strong  $d_{NN}(i, i + 1)$  between residues 16 and 17, 17 and 18, and 18 and 19 and weak  $d_{\alpha N}(i,$

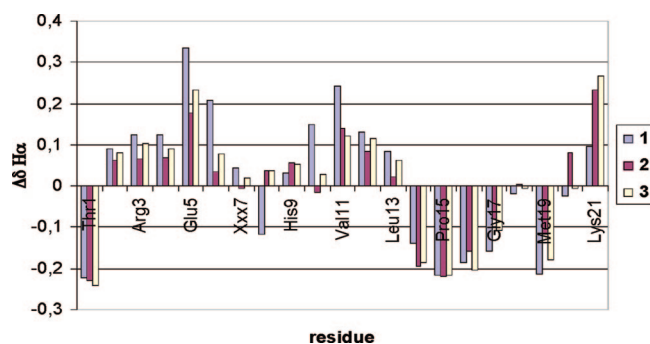


**Figure 2.** Plots of chemical shift deviations of  $H_{\alpha}$  protons from random-coil values in water/HFA (1/1 v/v) solution. Random-coil values were taken from ref 21b.

$i + 2$ ) among residues 16–18 and 17–19 are typical of nascent helix fragments in solution.<sup>22</sup>

With regard to the HFA/water sample solution, the better dispersion of the proton resonances indicates a higher structural definition in this environment. The presence of a  $\beta$ -turn that encompasses residues 6–9 is suggested by a weak  $H_{\alpha}$ – $NH_{i+2}$  connectivity between Pro<sup>7</sup> and His<sup>9</sup>. A turn structure is supported by the observation of a relatively more negative temperature coefficient of His<sup>9</sup> NH ( $\Delta\delta/\Delta T = -3.4$  ppb/K). Downfield shifts of  $H_{\alpha}$  resonance, relative to random-coil values (Figure 2), indicate that residues that flank the turn structure (2–5 and 10–13) are in an extended conformation whereas the upfield shifts in  $H_{\alpha}$  resonances of residues from Ala<sup>14</sup> to Met<sup>19</sup>, together with a continuum stretch of  $d_{\alpha N}(i, i + 2)$  and a few  $d_{\alpha\beta}(i, i + 3)$  and  $d_{\alpha N}(i, i + 4)$  NOEs in the same region, are consistent with a helical structure along this peptide segment.

For **2**, 157 NOE-derived distance constraints (66 intraresidue, 69 sequential, and 22 medium range; Supporting Information) were obtained in an HFA/water solution and were used as input for a restrained structure calculation using a simulating annealing protocol.<sup>23</sup> Figure 3a shows the 10 lowest-energy conformers of the 100 calculated structures. Structures are well defined in regions 6–9 and 15–19, with rmsd's of 0.5 and 0.3 Å, respectively, calculated over the backbone atoms. A type I  $\beta$ -turn that encompasses residues 6–9 is observed in most of the calculated structures (73/100). The two segments that involve residues 2–5 and 10–13 prefer an extended conformation and can be classified as  $\beta$ -strand regions. They are quite flexible because the rmsd of the 2–13 fragment increases to 1.2 Å. The two strands do not form an antiparallel  $\beta$ -sheet, but they diverge from each other. The type I  $\beta$ -turn structure and its flanking  $\beta$ -strand regions are evidenced in Figure 3b. In the same Figure, the Asn(Glc) moiety can be observed; it is well exposed to the solvent and to possible intermolecular contacts.

For peptide **3**, NMR analysis performed in water indicates disordered conformations. Only a very weak  $d_{\alpha N}(i, i + 2)$  NOE observed between Gly<sup>7</sup> and His<sup>9</sup> indicates the presence of a structure population that possesses a  $\beta$ -turn moiety that encompasses residues 6–9.

With regard to the HFA/water sample solution, the better dispersion of the proton resonances indicates a higher structural definition in this environment. Following arguments similar to those for peptide **2**, NMR data indicate the presence of a  $\beta$ -turn about residues 7 and 8, an extended conformation of the residues flanking the turn structure (2–5 and 10–13), and a helical structure at the C-terminal residues. A short stretch of antiparallel  $\beta$ -sheet involving residues 2–5 and 10–13 is inferred from nine interstrand NOEs including diagnostic  $d_{\alpha\alpha}(i, j)$ ,  $d_{\alpha N}(i, j)$ , and  $d_{NN}(i, j)$  connectivities. (See the Supporting Information).

Overall, 198 meaningful NOE-derived restraints (83 intraresidue, 85 sequential, 25 medium-range, and 5 long-range; Supporting Information) were used as input for the simulating annealing calculation. Figure 4a shows the 10 lowest-energy conformers out of the 100 calculated structures for glycopeptide **3**. Structures are well defined in regions 2–13 and 15–19 with rmsd's of 0.4 and 0.3, respectively, calculated over the backbone atoms. A short stretch of antiparallel  $\beta$ -sheet that involves residues 2–5 and 10–13 is observed together with a type II'  $\beta$ -turn that encompasses residues 6–9, and hence the peptide shows a  $\beta$ -hairpin structure with the Asn(Glc) moiety well exposed to the solvent and to possible intermolecular contacts (Figure 4b).

Peptide **4** shows spectral features ( $^3J_{HN-H\alpha}$  coupling constants,  $H_{\alpha}$  resonances, and temperature coefficients) that are very similar to those of the parent peptide **2** in both water and HFA/water solution. (See the Supporting Information.) The major difference observed in the spectra of **4** is the high intensity of signals that are attributable to the *cis*-proline isomer (about 20% of the total compared with 5% observed for peptide **2**). These signals overlap with some important NOE contacts in the NOESY spectrum of **4** such as the diagnostic  $d_{\alpha N}(i, i + 2)$  NOE between Gly<sup>7</sup> and His<sup>9</sup>. In any case, the similarity of other NMR parameters of **4** to the corresponding ones of **2** allows us to hypothesize the presence of the type I  $\beta$ -turn along residues 6–9 in glycopeptide **4** as well.

**Molecular Dynamics Simulations.** Restrained molecular dynamics simulations of glycopeptides **2** and **3** were conducted to determine whether the annealed structures adequately represented the peptides in solution. For each peptide, the starting structure was the lowest-energy annealed structure. The minimized structure was heated to 300 K, allowed to equilibrate for 1 ps, and permitted to move about for 10 ns. The simulation was performed in vacuo, and as a rough estimation of the solvent effects, a distance-dependent dielectric constant ( $\epsilon = 4r$ ) was used. We checked the stability of the  $\beta$ -turn structure by monitoring the backbone dihedral angle values of the central-turn residues 7 and 8. These dihedral angles are quite stable along the entire simulation time (Supporting Information, Figures S1–6). Furthermore, residues 2–6 and 9–13 reside in the  $\beta$ -region of the Ramachandran plot. Thus, we observe a good agreement between annealed and dynamic structures, and both can be considered to be good models to describe the conformational behavior of peptides **2** and **3** in solution.

## Discussion

In light of the importance of the conformation and of the correct exposure of epitopes involved in autoantibody recognition, we have recently studied synthetic glycopeptides that are able to recognize autoantibodies in MS patients' sera in an optimized solid-phase immunoenzymatic assay. In particular, we described glycopeptide **1** (Table 1), the first antigenic probe utilized to measure specific autoantibody titers in MS patients' sera as a disease biomarker.<sup>4</sup> The antigenic activity of glycopeptide **1** relies on the presence of an *N*-glycosylated asparagine residue located at the tip of a  $\beta$ -turn structure. In fact, a conformation–activity relationship study of **1** and of a focused library of glycopeptides bearing the same Asn(Glc)Gly sequence as **1** showed that peptides that are able to recognize autoantibodies have a type I'  $\beta$ -turn around the minimal epitope, that is, the Asn(Glc) residue.<sup>9</sup> To understand the role of the peptide structure in antibody recognition better, we have developed a new series of glycopeptides (**2–5**, Table 1) that are characterized by different  $\beta$ -turn types. According to the design strategy,

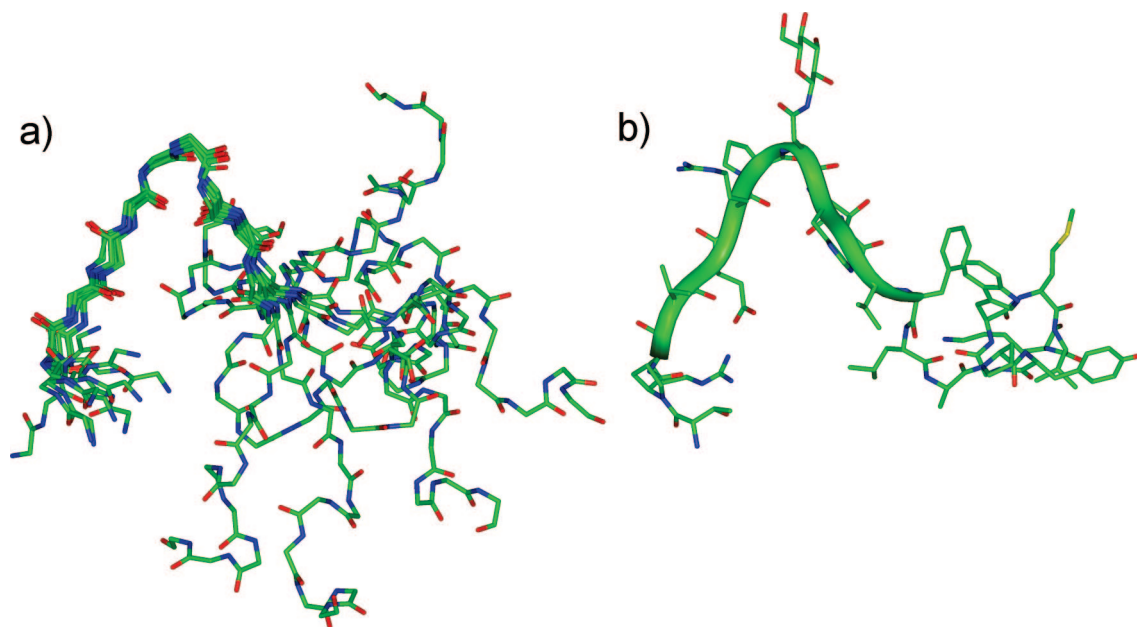


**Figure 3.** (a) Superposition of the 10 lowest-energy conformers of **2**. Structures were superimposed by the use of the backbone heavy atoms of residues 3–12 (thicker lines). Heavy atoms are shown in different colors. (Carbon, nitrogen, and oxygen are green, blue, and red, respectively.) For clarity, side chains and hydrogen atoms are not shown. (b) Lowest-energy conformer of **2**.  $\beta$ -turn and  $\beta$ -strand regions are evidenced as a ribbon.

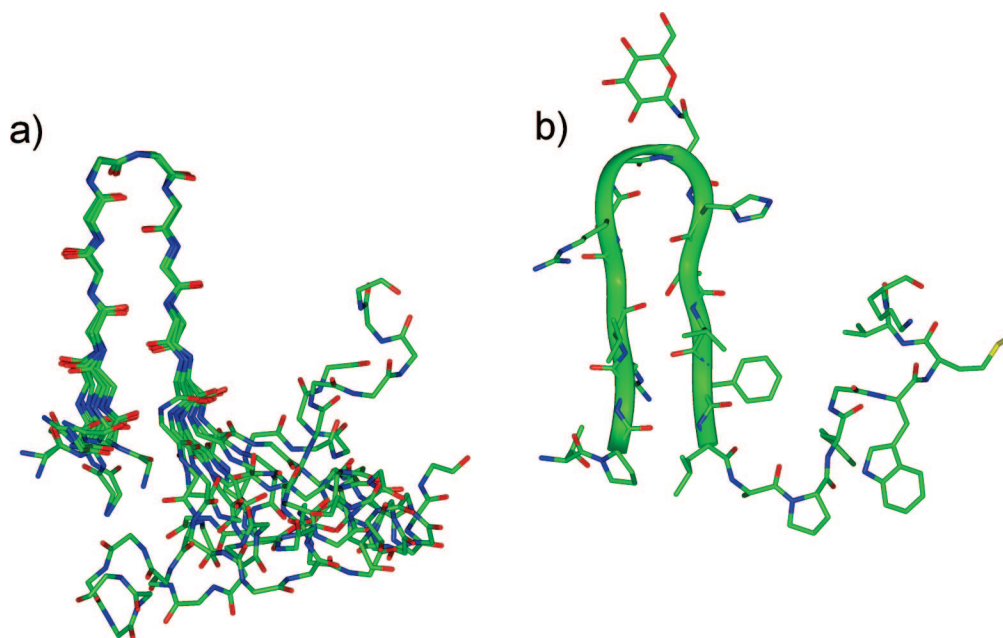


**Figure 4.** (a) Superposition of the 10 lowest-energy conformers of **3**. We superimposed the structures by using the backbone heavy atoms of residues 3–12 (thicker lines). Heavy atoms are shown in different colors. (Carbon, nitrogen, and oxygen are green, blue, and red, respectively.) For clarity, side chains and hydrogen atoms are not shown. (b) Lowest-energy conformer of **3**.  $\beta$ -hairpin structure is evidenced as a ribbon.

peptide **2** shows a type I  $\beta$ -turn motif around residues 6–9 (Figure 3), whereas peptide **3** shows a type II'  $\beta$ -turn motif around the same residues (Figure 4). In both cases, the residue Asn(Glc) is placed at position  $i + 2$  of the  $\beta$ -turn and is nicely exposed to antibody recognition. The designed peptides showed a high affinity for autoantibodies, and peptide **2** was 1 log unit more active than its precursor **1**. ( $IC_{50} = 11.8$  and  $137$  nM, respectively.) According to our experimental results, MS autoantibodies recognize glycopeptide structures on the order type I > type II' > type I'. A type I  $\beta$ -turn structure was already found in the crystal structure of other peptides in complex with antibodies.<sup>24,25</sup> Interestingly, the type I  $\beta$ -turn structure also increases the antibody affinity in shorter peptides **4** and **5** (Figure

1). The availability of these short, active peptides will make the systematic search for glycopeptides that are optimized for autoantibody recognition easier. Classical investigation methods such as Ala- and D-residue scans together with new NMR-based epitope mapping methods (STD NMR,<sup>26</sup> WaterLOGSY<sup>27</sup>) will be used for the determination of residues that are indispensable for antibody interaction.

## Conclusions

Our results confirm the role of conformation in the recognition and binding of synthetic antigenic probes to MS autoantibodies in the context of an immunoenzymatic assay (ELISA). Glycopeptide **2**, which is characterized by a type I  $\beta$ -turn around the

minimal epitope Asn(Glc), shows the highest antibody affinity; therefore, it appears to be a promising tool for the detection of specific autoantibodies as MS biomarkers in patients' sera for an early diagnosis, a better prognosis, and optimized therapy, and will thus contribute to a more effective management of MS.

## Experimental Section

**Chemistry: Materials and Methods.** Protected L-amino acids, Fmoc-Lys(Boc)-Wang resin, and Rink amide resin were purchased from Novabiochem (Läufelfingen, Switzerland). Peptide synthesis grade DMF was purchased from Scharlau (Barcelona, Spain), HOBt and TBTU were purchased from Iris Biotech (Marktredwitz, Germany), and TFA, DCM, piperidine, NMM, and DIPEA were purchased from Aldrich (Milan, Italy). We performed the characterization of the products via ultraperformance liquid chromatography on an ACQUITY UPLC (Waters Corporation, Milford, Massachusetts) coupled to a single-quadropole ESIMS (Micromass ZQ) using a ACQUITY BEH C18 column ( $2.1 \times 50$  mm<sup>2</sup>; 30 °C; flow rate, 0.45 mL/min) with an acetonitrile-water mobile phase containing TFA (0.1% v/v). All peptides were purified by semipreparative RPLC on a Waters model 600 system using a Jupiter C18 column ( $250 \times 10$  mm<sup>2</sup>) at 4 mL/min according to the methods described in Table 1 (Supporting Information). We analyzed the purity of the peptides by using a Waters Alliance (model 2695) HPLC system with a Jupiter Phenomenex column (C18, 200 Å,  $250 \times 4.6$  mm<sup>2</sup>) at 1 mL/min with a mixture of eluents: (a) 0.1% TFA in H<sub>2</sub>O (MilliQ) and (b) 0.1% TFA in CH<sub>3</sub>CN; UV detection, 254 nm.

**Peptide Synthesis.** Solid-phase peptide synthesis was performed on the Liberty microwave-assisted automatic peptide synthesizer (CEM, Matthews, NC), an additional module of CEM's Discover that combines microwave energy at 2450 MHz following the Fmoc/tBu strategy. Peptides **1–3** were prepared starting from a Fmoc-Lys(Boc)-Wang resin (0.67 mmol/g). Peptides **4** and **5** were prepared starting from a Rink amide resin (250 mg, 0.63 mmol/g). Each deprotection and coupling reaction was performed with microwave energy and nitrogen bubbling. Fmoc deprotections were performed with a 20% piperidine solution in DMF. Fmoc amino acids were stored as 0.3 M DMF solutions. The coupling reagent was predissolved in DMF (0.3 M solution). Coupling reactions were performed with 0.25 M TBTU/DMF (2.5 equiv), 0.1 M amino acid/DMF (2.5 equiv), and 0.7 M DIPEA/NMP (3.5 equiv). Fmoc-L-Asn(GlcAc<sub>4</sub>)OH (2.5 equiv) that was synthesized as previously reported<sup>13</sup> was coupled using HOBt (1.5 equiv), TBTU (1.5 equiv), and NMM (3 equiv) in DMF for 1.5 h. Deprotection and coupling reactions were performed with microwave energy and nitrogen mixing. The microwave cycle was characterized by two deprotection steps (30 and 180 s). All microwave coupling reactions were performed for 300 s at 75 °C. We achieved the acetylation of peptides **4** and **5** by treating the resin with a mixture of acetic anhydride (20 equiv), NMM (20 equiv), and DMF for 5 min and repeating for 30 min. After the synthesis of each glycopeptide was complete, the peptidyl resins were washed with DMF and DCM and were dried under vacuum prior to cleavage. The cleavage from the resin and side-chain deprotection of peptides **1–3** was performed by the use of a TFA/thioanisole/EDT/phenol/H<sub>2</sub>O mixture (94/2/2/2/2 v/v/v/v/v) (reagent K). The cleavage from the resin and side-chain deprotection of peptides **4** and **5** was carried out with TFA/TIS/H<sub>2</sub>O (96/2/2). The resin was treated for 2.5 h with reagent K (1 mL/100 mg of resin) at room temperature. The resin was filtered off, and the solution was concentrated by flushing with nitrogen. The peptides were precipitated from cold Et<sub>2</sub>O/diisopropyl ether, were centrifuged, and were lyophilized. The deprotection of the hydroxyl functions of sugar moieties linked to peptides **1–5** was performed by the addition of 0.1 M methanolic NaOMe solution to a solution of the lyophilized peptides in dry MeOH (1 mL/100 mg of resin) until pH 12 was reached. After 3 h, the reaction was quenched by the addition of concentrated HCl until pH 7 was reached; the solvent was evaporated under vacuum, and the residue

was lyophilized. Peptides were purified and characterized as described above (Table 1; Supporting Information).

**Immunoenzymatic Assay.** Sera were obtained for diagnostic purposes from patients who had given their informed consent and were stored at -20 °C until use. The antibody affinity was measured according to Rath et al.<sup>14</sup> In pure carbonate buffer (0.05 M, pH 9.6), 96-well polystyrene ELISA plates (Nunc Maxisorp, Sigma) were coated with 1 µg/100 µL of glycopeptides per well and were incubated at 4 °C overnight. The semisaturating sera dilution (1/600) was calculated from preliminary titration curves (absorbance, 0.7). At this dilution, sera were preincubated with increasing synthetic-peptide antigen concentrations ( $0, 3.84 \times 10^{-11}, 3.84 \times 10^{-10}, 3.84 \times 10^{-9}, 3.84 \times 10^{-8}, 3.84 \times 10^{-7}, 3.84 \times 10^{-6}$ , and  $1.92 \times 10^{-5}$ ) for 1 h at room temperature. Unblocked antibodies were revealed by ELISA as follows: after the plates were washed five times with saline containing 0.05% Tween 20, we added to each well 100 µL of alkaline-phosphatase-conjugated antihuman IgG (diluted 1/8000 in saline/0.05% Tween 20/10% FCS, Sigma). After the plates were incubated for 3 h at room temperature and were washed five times, 100 µL of a substrate solution consisting of 1 mg/mL *p*-nitrophenyl phosphate (Sigma) in 10% diethanolamine buffer was applied. After 30 min, the reaction was stopped with 1 M NaOH (50 µL), and the absorbance was read in a multichannel ELISA reader (Tecan Sunrise) at 405 nm. ELISA plates, coating conditions, reagent dilutions, buffers, and incubation times were tested in preliminary experiments.<sup>4</sup> The antibody levels are expressed as absorbance in arbitrary units at 405 nm, and the antigenic probe concentration versus the percent absorbance is presented graphically.

**Nuclear Magnetic Resonance Spectroscopy.** HFA and 99.9% D<sub>2</sub>O were obtained from Aldrich (Milwaukee), and TSP was obtained from MSD Isotopes (Montreal). We prepared the samples for NMR spectroscopy by dissolving the appropriate amount of peptides in 0.45 mL of <sup>1</sup>H<sub>2</sub>O (pH 5.0) and 0.05 mL of <sup>2</sup>H<sub>2</sub>O or in 0.20 mL of <sup>1</sup>H<sub>2</sub>O, 0.05 mL of <sup>2</sup>H<sub>2</sub>O, and 0.25 mL of HFA; 1 to 2 mM solutions were obtained. TSP was used as an internal chemical shift standard. The experiments were carried out on a Varian UnityInova spectrometer that was operating at a 700 MHz proton resonance frequency and was equipped with triple-resonance cryo-cooled HCN probes and shielded z-gradient coils. The spectra in water were recorded at 277.1 K, and the spectra in the water/HFA solution were recorded at 300 K. The spectra were calibrated relative to TSP (0.00 ppm) as an internal standard. 1D NMR spectra were recorded in the Fourier mode with quadrature detection. The water signal was suppressed by a gradient echo.<sup>28</sup> 2D DQF-COSY,<sup>17</sup> TOCSY,<sup>18</sup> and NOESY<sup>19</sup> spectra were recorded in the phase-sensitive mode by the use of the method from States.<sup>29</sup> Typical data block sizes were 2048 addresses in t<sub>2</sub> and 512 equidistant t<sub>1</sub> values. Before Fourier transformation, the time-domain data matrices were multiplied by shifted sin<sup>2</sup> functions in both dimensions. A mixing time of 70 ms was used for the TOCSY experiments. NOESY experiments were run with mixing times in the range of 150–300 ms. We obtained the qualitative and quantitative analyses of DQF-COSY, TOCSY, and NOESY spectra by using the interactive program package XEASY.<sup>20,3</sup> <sup>J</sup><sub>HN-Hα</sub> coupling constants were obtained from 1D <sup>1</sup>H NMR and 2D DQF-COSY spectra. The temperature coefficients of the amide proton chemical shifts were calculated by means of linear regression from 1D <sup>1</sup>H NMR and 2D DQF-COSY experiments that were performed at different temperatures in the range of 300–320 K for the water/HFA solution and 277–280 K for water solutions.

**Structural Determinations and Computational Modeling.** The NOE-based distance restraints were obtained from NOESY spectra that were collected with a mixing time of 200 ms. The NOE cross peaks were integrated with the XEASY program and were converted into upper distance bounds by the use of the CALIBA program incorporated into the program package DYANA.<sup>23</sup> Cross peaks, which were more than 50% overlapped, were treated as weak restraints in the DYANA calculation. Only NOE-derived constraints were considered in the annealing procedures. For each examined peptide, an ensemble of 200 structures was generated by the

simulated annealing of DYANA. An error-tolerant target function (tf type 3) was used to account for the peptide intrinsic flexibility. We added a nonstandard Asn(Glc) residue to the DYANA residue library by using MOLMOL.<sup>30</sup> From the 200 structures, we chose 50 whose interprotonic distances best fit the NOE-derived distances, and we then refined the structures through successive steps of restrained and unrestrained energy minimization calculations by using the Discover algorithm (Accelrys, San Diego) and the consistent valence force field (CVFF).<sup>31</sup> No residue was found in the disallowed region of the Ramachandran plot. We analyzed the final structures by using the InsightII program (Accelrys, San Diego), which was the same program that was used for the graphical representations. By using the MOLMOL program, we carried out rms deviation analyses between energy-minimized structures.<sup>30</sup> The PROMOTIF program was used to extract details on the location and types of structural secondary motifs.<sup>32</sup>

**Molecular Dynamics Simulation.** We subjected peptides **2** and **3** to a molecular dynamics simulation by using the Discover algorithm (Biosym, San Diego, CA) that utilized the CVFF.<sup>31</sup> The lower-energy conformer that we obtained from the annealing simulation by following the minimization procedures described above was subjected to 10 ns of molecular dynamics calculations after an equilibration period of 1 ps at 300 K. During the molecular dynamics frame, structures were saved every 1 ps. A distance-dependent dielectric constant that was equal to  $4r$  was applied so that we could evaluate electrostatic interactions. Force constants for distance restraints were  $16 \text{ kcal}/(\text{mol} \cdot \text{Å}^2)$ .

**Acknowledgment.** We thank the Fondazione Ente Cassa di Risparmio di Firenze (Italy) for the financial support to the Laboratory of Peptide and Protein Chemistry and Biology of the University of Florence. This work was partially funded by PRIN 2005 (Ministero dell'Università e della Ricerca, prot. 2005032959).

**Supporting Information Available:** Analytical and NMR data of the analyzed peptides, HPLC and ESIMS profiles of selected compounds, distance restraint lists, and details of the MD simulations. This material is available free of charge via the Internet at <http://pubs.acs.org>.

## References

- (1) Leslie, D.; Lipsky, P.; Notkins, A. L. Autoantibodies as Predictors of Disease. *J. Clin. Invest.* **2001**, *108*, 1417–1422.
- (2) Mahler, M.; Blüthner, M.; Pollard, K. M. Advances in B-Cell Epitope Analysis of Autoantigens in Connective Tissue Diseases. *Clin. Immunol.* **2003**, *107*, 65–79.
- (3) Leung, P. S. C.; Gershwin, M. E. Native Autoantigens Versus Recombinant Autoantigens. In *Autoantibodies*, 2nd ed.; Shoenfeld, Y., Gershwin, M. E., Meroni, P. L., Eds.; Elsevier: Boston, 2007; pp 37–45.
- (4) Lolli, F.; Mulinacci, B.; Carotenuto, A.; Bonetti, B.; Sabatino, G.; Mazzanti, B.; D'Ursi, A. M.; Novellino, E.; Pazzagli, M.; Lovato, L.; Alcaro, M. C.; Peroni, E.; Pozo-Carrero, M. C.; Nuti, F.; Battistini, L.; Borsellino, G.; Chelli, M.; Rovero, P.; Papini, A. M. An *N*-Glucosylated Peptide Detecting Disease-Specific Autoantibodies, Biomarkers of Multiple Sclerosis. *Proc. Natl. Acad. Sci. U.S.A.* **2005**, *102*, 10273–10278.
- (5) Thompson, A. J. Clinical Review of Multiple Sclerosis. *Clin. Immunother.* **1996**, *5*, 1–11.
- (6) Doyle, H. A.; Mamula, M. J. Post-Translational Protein Modifications in Antigen Recognition and Autoimmunity. *Trends Immunol.* **2001**, *22*, 443–449.
- (7) Alcaro, M. C.; Lolli, F.; Migliorini, P.; Chelli, M.; Rovero, P.; Papini, A. M. Peptides as Autoimmune Diseases Antigenic Probes: A Peptide-Based Reverse Approach to Detect Biomarkers of Autoimmune Diseases. *Chem. Today* **2007**, *25*, 14–16.
- (8) Lolli, F.; Mazzanti, B.; Pazzagli, M.; Peroni, E.; Alcaro, M. C.; Sabatino, G.; Lanzillo, R.; Brescia Morra, V.; Santoro, L.; Gasperini, C.; Galgani, S.; D'Elia, M. M.; Zipoli, V.; Sotgiu, S.; Pugliatti, M.; Rovero, P.; Chelli, M.; Papini, A. M. The Glycopeptide CSF114(Glc) Detects Serum Antibodies in Multiple Sclerosis. *J. Neuroimmunol.* **2005**, *167*, 131–137.
- (9) Carotenuto, A.; D'Ursi, A. M.; Mulinacci, B.; Paolini, I.; Lolli, F.; Papini, A. M.; Novellino, E.; Rovero, P. Conformation–Activity Relationship of Designed Glycopeptides as Synthetic Probes for the

Detection of Autoantibodies, Biomarkers of Multiple Sclerosis. *J. Med. Chem.* **2006**, *49*, 5072–5079.

- (10) Guruprasad, K.; Rajkumar, S.  $\beta$ - and  $\gamma$ -Turns in Proteins Revisited: A New Set of Amino Acid Turn-Type Dependent Positional Preferences and Potentials. *J. Biosci.* **2000**, *25*, 143–156.
- (11) Rizzolo, F.; Sabatino, G.; Chelli, M.; Rovero, P.; Papini, A. M. A Convenient Microwave-Enhanced Solid-Phase Synthesis of Difficult Peptide Sequences: Case Study of Gramicidin A and CSF114(Glc). *Int. J. Pept. Res. Ther.* **2007**, *13*, 203–208.
- (12) Real Fernández, F.; Colson, A.; Bayardon, J.; Nuti, F.; Peroni, E.; Meunier-Prest, R.; Lolli, F.; Chelli, M.; Darcel, C.; Jugé, S.; Papini, A. M. Ferrocenyl Glycopeptides as Electrochemical Probes to Detect Autoantibodies in Multiple Sclerosis Patients' Sera. *Biopolymers* **2008**, *90*, 488–495.
- (13) Paolini, I.; Nuti, F.; Pozo-Carrero, M. C.; Barbetti, F.; Kolesinska, B.; Kaminski, Z. J.; Chelli, M.; Papini, A. M. A Convenient Microwave-Assisted Synthesis of *N*-Glycosyl Amino Acids. *Tetrahedron Lett.* **2007**, *48*, 2901–2904.
- (14) Rath, S.; Stanley, C. M.; Steward, M. N. An Inhibition Enzyme Immunoassay for Estimating Relative Antibody Affinity and Affinity Heterogeneity. *J. Immunol. Methods* **1988**, *106*, 245–249.
- (15) Rajan, R.; Awasthi, S. K.; Bhattacharjya, S.; Balaram, P. "Teflon-Coated Peptides": Hexafluoroacetone Trihydrate as a Structure Stabilizer for Peptides. *Biopolymers* **1997**, *42*, 125–128.
- (16) Wüthrich, K. *NMR of Proteins and Nucleic Acids*; Wiley: New York, 1986.
- (17) (a) Piantini, U.; Sorensen, O. W.; Ernst, R. R. Multiple Quantum Filters for Elucidating NMR Coupling Networks. *J. Am. Chem. Soc.* **1982**, *104*, 6800–6801. (b) Marion, D.; Wüthrich, K. Application of Phase Sensitive Two-Dimensional Correlated Spectroscopy (COSY) for Measurements of  $^1\text{H}$ - $^1\text{H}$  Spin-Spin Coupling Constants in Proteins. *Biochem. Biophys. Res. Commun.* **1983**, *113*, 967–974.
- (18) Braunschweiler, L.; Ernst, R. R. Coherence Transfer by Isotropic Mixing: Application to Proton Correlation Spectroscopy. *J. Magn. Reson.* **1983**, *53*, 521–528.
- (19) Jenner, J.; Meier, B. H.; Bachman, P.; Ernst, R. R. Investigation of Exchange Processes by Two-Dimensional NMR Spectroscopy. *J. Chem. Phys.* **1979**, *71*, 4546–4553.
- (20) Bartels, C.; Xia, T.-h.; Billeter, M.; Güntert, P.; Wüthrich, K. The Program XEASY for Computer-Supported NMR Spectral Analysis of Biological Macromolecules. *J. Biomol. NMR* **1995**, *6*, 1–10.
- (21) (a) Wishart, D. S.; Sykes, B. D.; Richards, F. M. The Chemical Shift Index: A Fast and Simple Method for the Assignment of Protein Secondary Structure through NMR Spectroscopy. *Biochemistry* **1992**, *31*, 1647–1651. (b) Andersen, N. H.; Liu, Z.; Prickett, K. S. Efforts Toward Deriving the CD Spectrum of a  $3_{10}$  Helix in Aqueous Medium. *FEBS Lett.* **1996**, *399*, 47–52.
- (22) Wishart, D. S.; Sykes, B. D.; Richards, F. M. Relationship between Nuclear Magnetic Resonance Chemical Shift and Protein Secondary Structure. *J. Mol. Biol.* **1991**, *222*, 311–333.
- (23) Güntert, P.; Mumenthaler, C.; Wüthrich, K. Torsion Angle Dynamics for NMR Structure Calculation with the New Program DYANA. *J. Mol. Biol.* **1997**, *273*, 283–298.
- (24) Derrick, J. P.; Maiden, M. C. J.; Feavers, I. M. Crystal Structure of an Fab Fragment in Complex with a Meningococcal Serosubtype Antigen and a Protein G Domain. *J. Mol. Biol.* **1999**, *293*, 81–91.
- (25) Oomen, C. J.; Hoogerhout, P.; Kuipers, B.; Vidarsson, G.; van Alphen, L.; Gros, P. Crystal Structure of an Anti-Meningococcal Subtype P1.4 PorA Antibody Provides Basis for Peptide–Vaccine Design. *J. Mol. Biol.* **2005**, *351*, 1070–1080.
- (26) Mayer, M.; Meyer, B. Group Epitope Mapping by Saturation Transfer Difference NMR to Identify Segments of a Ligand in Direct Contact with a Protein Receptor. *J. Am. Chem. Soc.* **2001**, *123*, 6108–6117.
- (27) Dalvit, C.; Fogliatto, G.; Stewart, A.; Veronesi, M.; Stockman, B. WaterLOGSY as a Method for Primary NMR Screening: Practical Aspects and Range of Applicability. *J. Biomol. NMR* **2001**, *21*, 349–359.
- (28) Hwang, T. L.; Shaka, A. J. Water Suppression that Works: Excitation Sculpting Using Arbitrary Wave-Forms and Pulsed-Field Gradients. *J. Magn. Reson.* **1995**, *112*, 275–279.
- (29) States, D. J.; Haberkorn, R. A.; Ruben, D. J. A Two-Dimensional Nuclear Overhauser Experiment with Pure Absorption Phase Four Quadrants. *J. Magn. Reson.* **1982**, *48*, 286–292.
- (30) Koradi, R.; Billeter, M.; Wüthrich, K. MOLMOL: A Program for Display and Analysis of Macromolecular Structures. *J. Mol. Graphics* **1996**, *14*, 51–55.
- (31) Maple, J.; Dinur, U.; Hagler, A. T. Derivation of Force Fields for Molecular Mechanics and Dynamics from Ab Initio Energy Surface. *Proc. Natl. Acad. Sci. U.S.A.* **1988**, *85*, 5350–5354.
- (32) Hutchinson, E. G.; Thornton, J. M. PROMOTIF: A Program to Identify and Analyze Structural Motifs in Proteins. *Protein Sci.* **1996**, *5*, 212–220.